



# ANTIFERROMAGNETISM

— 1936 —



# ANTIFERROMAGNETISM

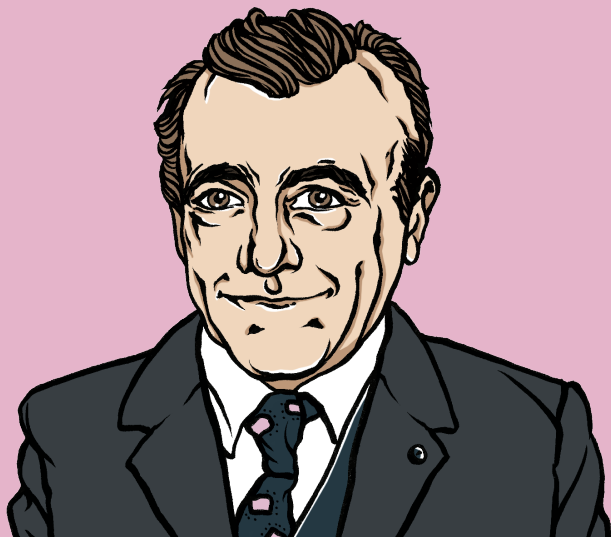


INSTITUT DE PHYSIQUE DE STRASBOURG, FRANCE



# ANTIFERROMAGNETISM

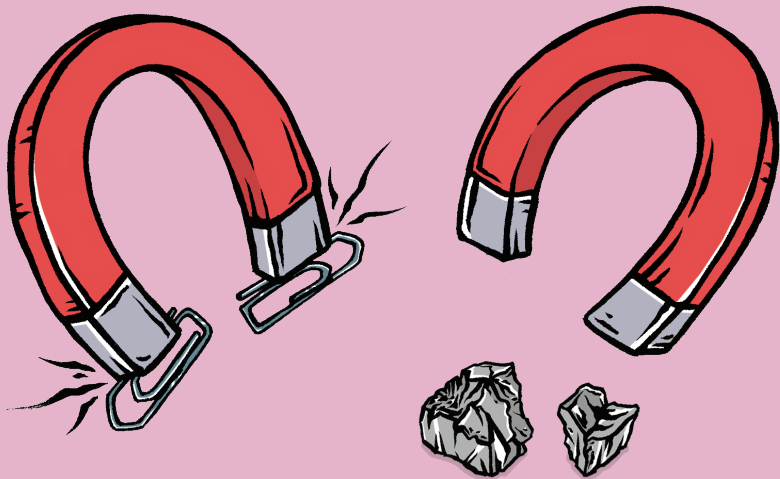




L. NÉEL



# ANTIFERROMAGNETISM

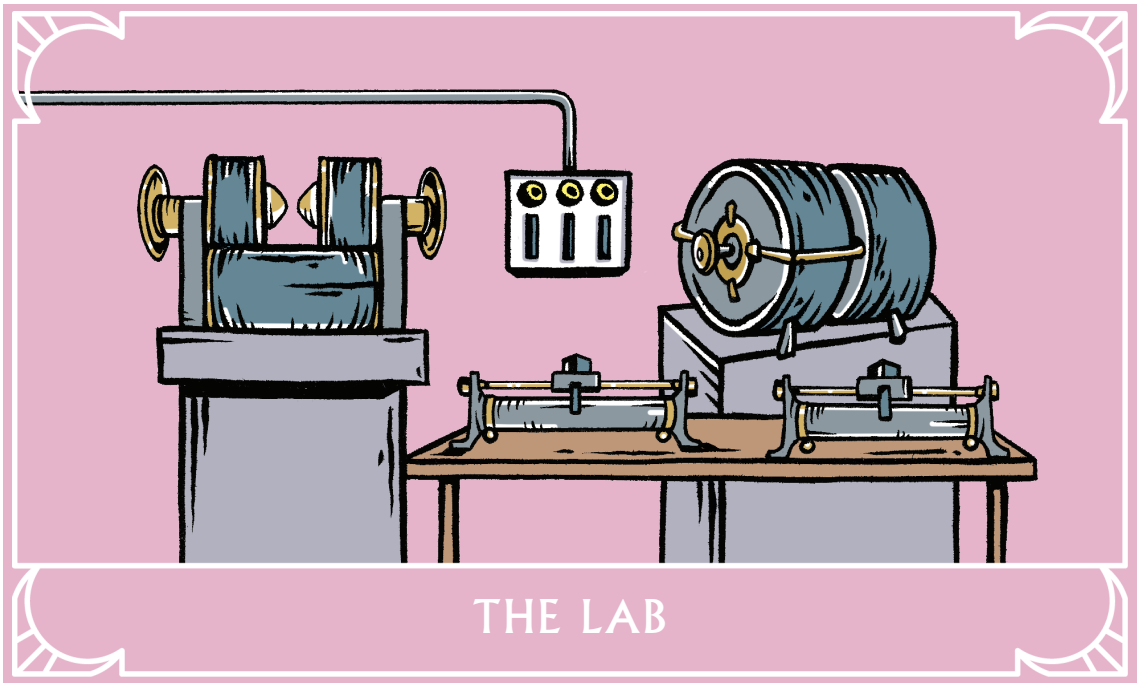


## THE QUESTION

Why some metals or oxides such as chromium do not seem to display any magnetism?



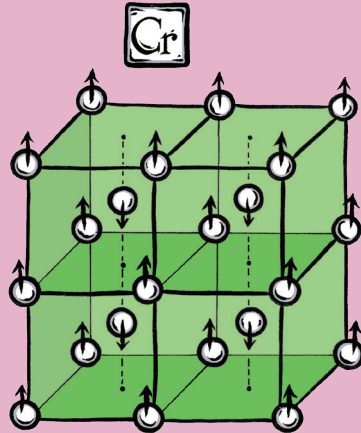
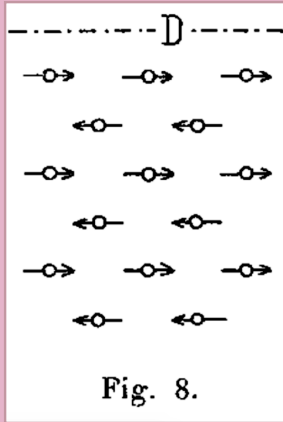
# ANTIFERROMAGNETISM



THE LAB



# ANTIFERROMAGNETISM



## THE RESULT

In some metals and oxides, the atoms carry small magnets called spins which order antiparallel to each other. These antiferromagnets do not show poles as in real magnets even though they too display a long range order.



# ANTIFERROMAGNETISM



PROPRIÉTÉS MAGNÉTIQUES  
DE L'ÉTAT MÉTALLIQUE ET ÉNERGIE  
D'INTERACTION ENTRE ATOMES  
MAGNÉTIQUES

Par M. LOUIS NÉEL

SOMMAIRE. — Une première partie du travail (§ 1 à 10) est consacrée à l'interprétation des expériences de M. Manders sur les variations, en fonction de la température, de la susceptibilité magnétique de quelques solutions solides à base de nickel (Ni et Al) ou de Ti, Sn, Sb, V, Mo, W, Cr). On étudie et on interprète les variations, en fonction du titre, de la constante de Curie et du coefficient de paramagnétisme constant superposé. On en déduit que les électrons magnétiques du nickel restent en nombre constant lorsqu'on passe de l'état ferro à l'état paramagnétique.

Dans une deuxième partie (§ 11 à 29), on expose comment on peut définir et calculer une énergie d'interaction magnétique entre deux atomes voisins porteurs de moment, à partir des données expérimentales, soit pour les ferromagnétiques, soit pour les corps à champ moléculaire négatif (Pd et Pt), soit pour les corps paramagnétiques à susceptibilité indépendante de la température (Mn, Cr, Ti, Mo, Ru, Rh, etc.). On étudie ensuite les variations de l'énergie d'interaction avec la distance entre les couches magnétiques des atomes interagissant et on montre qu'en première approximation l'énergie d'interaction ne dépend que de cette distance et varie très régulièrement avec elle. Cette conception permet d'interpréter et de relier entre eux un certain nombre de faits expérimentaux dont quelques-uns sont passés en revue.

Enfin, en supposant qu'il existe un couplage entre le réseau cristallin et les spins responsables du magnétisme des métaux, apparaissent des propriétés curieuses qui semblent être un point de départ pour expliquer les propriétés magnétiques compliquées du platine (§ 18, 19 et 20).

§ 16. Calcul de  $\omega_{AB}$  d'après les données expérimentales. — Si la concentration du métal B est petite, on a :

$$V = P\alpha_1 + Q \frac{\theta}{\alpha} C_0 \quad \text{et} \quad C' = PC_0 + QC_0 \left( \frac{\theta}{\alpha} - \frac{\theta'}{\alpha'} \right) \quad (11)$$

soit, en fonction du titre, une variation linéaire du point de Curie et de la constante de Curie apparente. Prolongeons les droites obtenues jusqu'à  $Q = 1$  ; soit  $\theta'$  et  $C'$  les valeurs de  $\theta$  et  $C'$  correspondant à  $Q = 1$ , d'après (11) on a :

$$\frac{C'}{\theta'} = \frac{\theta}{\alpha} - \frac{1}{\alpha} \quad \text{ou} \quad b = \frac{\theta}{\theta'} + \frac{1}{\alpha} \quad (12)$$

en remarquant que pour le métal A pur, de constante de Curie  $C_A$  et de point de Curie  $\theta_A$ , on a :  $a = \frac{\theta_A}{C_A}$ .  $C'$  et  $\theta'$  se déterminent expérimentalement en extrapolant les tangentes initiales aux courbes de variation de la constante de Curie et du point de Curie en fonction du titre. J'ai appliqué cette méthode pour calculer les énergies d'interaction des liaisons mixtes  $\omega_{AB}$  : Ni-Co, Ni-Fe, Co-Fe, d'après les données expérimentales de Preuss (10), de Foschard (11) et de Bloch (14).

Dans le calcul précédent,  $\omega_{AB}$  représente l'énergie totale d'interaction entre deux moments  $\mu_A$  et  $\mu_B$ . Pour avoir des valeurs comparables aux  $\omega$  du § 14, il faut exprimer  $\omega_{AB}$  au moyen de l'énergie  $\omega_{AB}$  d'interaction de deux électrons, portés l'un par l'atome A et l'autre par l'atome B. Posons  $\mu_A = g\mu_B$ ,  $\mu_B = g'\mu_B$  en désignant par  $\mu_B$  le magnéton de Bohr. On a immédiatement :  $\omega_{AB} = gg'\omega_{AB}$ . D'où, d'après la formule 8, puisque le facteur  $gg'$  disparaît haut et bas :

$$b = \frac{\omega_{AB}}{N\mu_B^2} \quad (13)$$

Le tableau 5 donne les valeurs de  $C'$ ,  $\theta'$ ,  $\omega_{AB}$  correspondant à différentes liaisons. Le système cristallin étant le cube à faces centrées, on a toujours :  $\alpha\mu = 12$ .

région où la formule 3 n'est pas valable, d'où la nécessité d'une étude spéciale de cette région qui sera pour les corps



Fig. 8.

à champ moléculaire négatif la réplique de la région ferromagnétique des corps à champ moléculaire positif.

Au zéro absolu, chaque atome se dispose antiparallèlement à ses voisins, de manière à réaliser un assemblage d'énergie

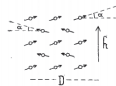


Fig. 9.

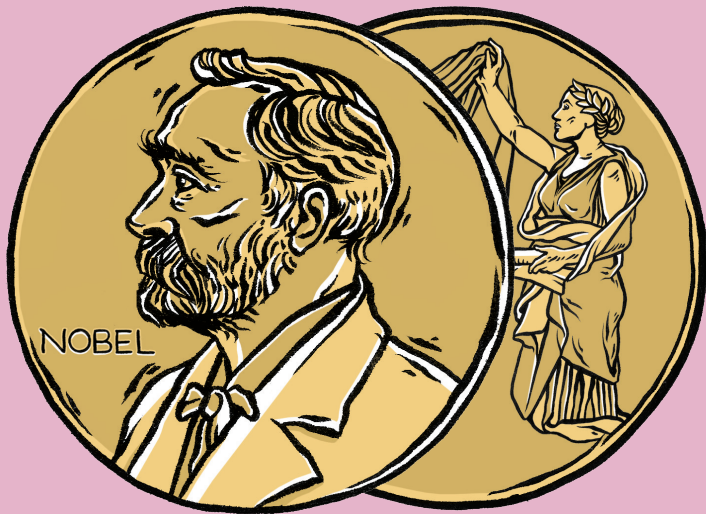
potentielle minimum comme celui qui est représenté sur la figure 8. Les moments sont tous parallèles à une même direction D, mais ils sont dirigés dans des sens différents au lieu d'être tous de même sens comme dans les ferromagnétiques. Un champ magnétique  $H$ , perpendiculaire à la direction D, va déformer cet assemblage et l'aîmanteur. Tous les

# THE ARTICLE

Propriétés magnétiques de l'état métallique et énergie d'interaction  
entre atomes magnétiques, L. Néel, Annales de Physique, 5, 232 (1936)



# ANTIFERROMAGNETISM

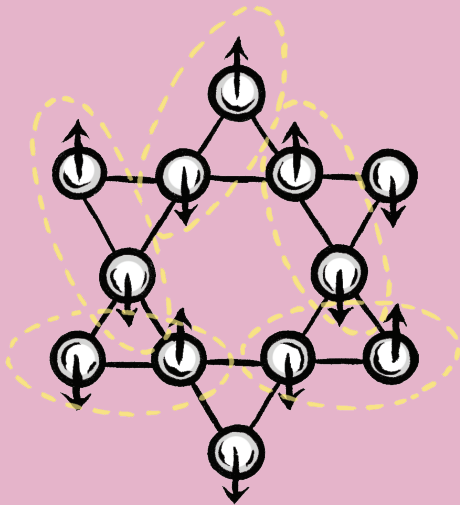


## NOBEL PRIZE, 1970

For fundamental work and discoveries concerning antiferromagnetism and ferrimagnetism which have led to important applications in solid state physics.



# ANTIFERROMAGNETISM



## NOWADAYS

The study of magnetism in solids is still a lively research field. For example, new “spin liquid” states have been recently discovered in solids which display star structures in which spins cannot order even close to absolute zero.



# ANTIFERROMAGNETISM



# GRAPHENE

— 2004 —



GRAPHENE





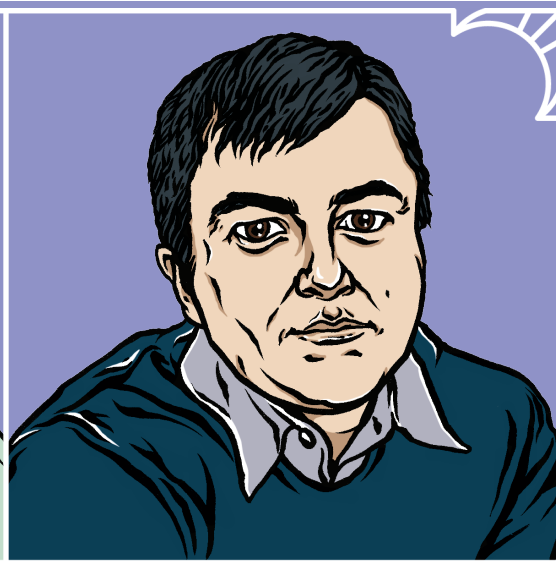
MANCHESTER UNIVERSITY, GREAT BRITAIN



GRAPHENE



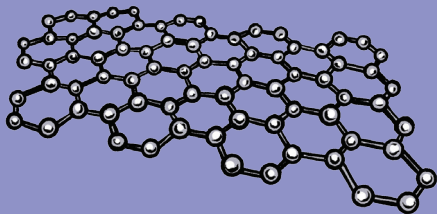
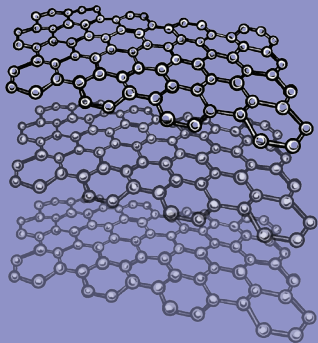
A. GEIM



K. NOVOSELOV



GRAPHENE

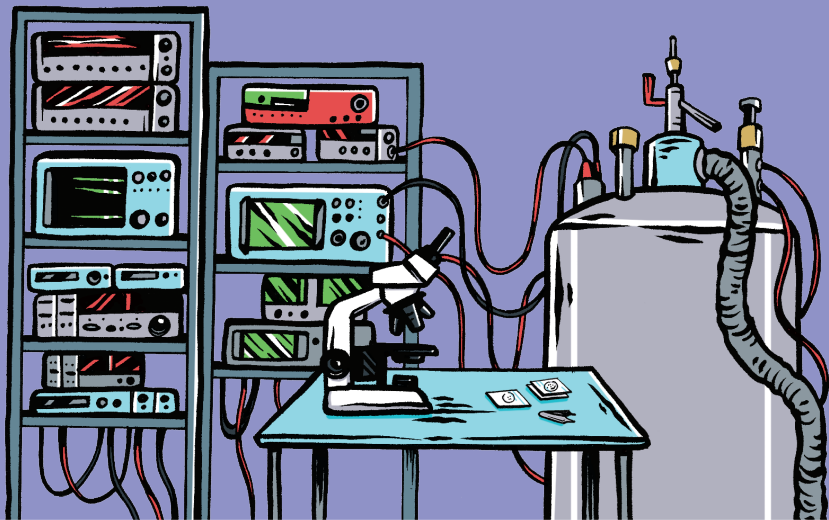


## THE QUESTION

Could one create a material made of a single layer of carbon atoms from graphite?  
What would be its properties?



GRAPHENE

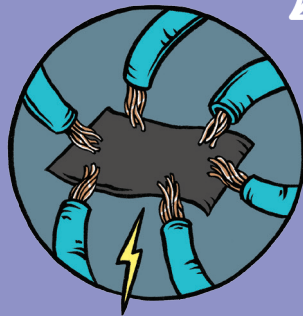
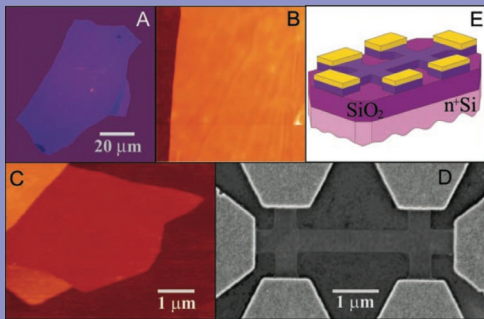


THE LAB



GRAPHENE





## THE RESULT

It is possible to create graphene, a 2 dimensions material of a single atom thick. Its mechanical properties are remarkable, and its electrical properties are surprising: neither an insulator nor a metal.



GRAPHENE

**REPORTS**

**Fig. 1. Conductance modulation (CM)** to show the field-effect on the  $g_{\text{min}}$  (green) and  $g_{\text{max}}$  (red) of the signal (blue) in the  $\mu\text{C}$  gate of the device. The inset shows the  $g_{\text{min}}$  and  $g_{\text{max}}$  versus the voltage of the  $\mu\text{C}$  gate at constant carrier densities.

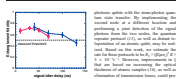


**Fig. 2. Time-dependent magnetotransport stability** of the signal and the  $g_{\text{min}}$  and  $g_{\text{max}}$  at  $10^6 \text{ V/m}$  for the  $\mu\text{C}$  gate.

carrier efficiency for the read time is  $\approx 0.2$ , which is one order of magnitude of quantum state transfer from the atoms into the photoconductor (12).

We have realized a quantum gate by controlling the magnetotransport of atomic and

**Electric Field Effect in Atomically Thin Carbon Films**

K. S. Novoselov,<sup>1</sup> A. K. Geim,<sup>1</sup> S. V. Morozov,<sup>2</sup> D. Jiang,<sup>1</sup> Y. Zhang,<sup>1</sup> S. V. Dubonos,<sup>1</sup> I. V. Grigorieva,<sup>1</sup> A. A. Firsiroti<sup>1</sup>

We describe nonmetallic graphitic films, which are a new carbon allotrope that are unambiguously stable under ambient conditions, consisting of atomically thin graphite layers. The films are based on the idea of dimensional reduction of a single atomic sheet of graphite to a single atomic surface by intercalation up to 100% pore saturation with water vapor. Graphite membranes with controlled porosity can be used as a quantum gate.

The ability to control electronic properties of a material by externally applied fields is at the heart of modern electronics. In many cases, it is the electric field effect that allows one to vary the carrier concentration in a semiconductor device and, consequently, change an electric current through it. In the

<sup>1</sup>Department of Physics, University of Manchester, Oxford Road, Manchester M13 9PL, United Kingdom  
<sup>2</sup>Department of Physics, University of Cambridge, Cavendish Laboratory, Madingley Road, Cambridge CB3 0HJ, United Kingdom

semiconductor industry, it is using the field effect to control carrier concentrations in thin silicon layers (13). Graphene is a two-dimensional material that has been predicted to be a zero-gap semiconductor (14). It is a unique material because its carrier concentration can be controlled by the electric field. The most striking example of this is the quantum Hall effect (15), which is observed in a two-dimensional system of massless Dirac fermions (16).

One of the most interesting properties of graphene is the absence of a band gap (17). This means that it is a semimetal, and it is expected to have a zero band gap. This is in contrast to most other two-dimensional materials, which have a band gap. The absence of a band gap is a result of the unique geometry of the Dirac cones in graphene, which are separated by a  $2\pi$  phase shift.

Graphene has a unique band structure, which is a result of the unique geometry of the Dirac cones. The Dirac cones are separated by a  $2\pi$  phase shift, which results in a zero band gap. This is in contrast to most other two-dimensional materials, which have a band gap.

**REPORTS**

**Fig. 3. Conductance modulation (CM)** to show the field-effect on the  $g_{\text{min}}$  (green) and  $g_{\text{max}}$  (red) of the signal (blue) in the  $\mu\text{C}$  gate of the device. The inset shows the  $g_{\text{min}}$  and  $g_{\text{max}}$  versus the voltage of the  $\mu\text{C}$  gate at constant carrier densities.



**Fig. 4. Time-dependent magnetotransport stability** of the signal and the  $g_{\text{min}}$  and  $g_{\text{max}}$  at  $10^6 \text{ V/m}$  for the  $\mu\text{C}$  gate.

carrier efficiency for the read time is  $\approx 0.2$ , which is one order of magnitude of quantum state transfer from the atoms into the photoconductor (12).

We have realized a quantum gate by controlling the magnetotransport of atomic and

**Electric Field Effect in Atomically Thin Carbon Films**

K. S. Novoselov,<sup>1</sup> A. K. Geim,<sup>1</sup> S. V. Morozov,<sup>2</sup> D. Jiang,<sup>1</sup> Y. Zhang,<sup>1</sup> S. V. Dubonos,<sup>1</sup> I. V. Grigorieva,<sup>1</sup> A. A. Firsiroti<sup>1</sup>

We describe nonmetallic graphitic films, which are a new carbon allotrope that are unambiguously stable under ambient conditions, consisting of atomically thin graphite layers. The films are based on the idea of dimensional reduction of a single atomic sheet of graphite to a single atomic surface by intercalation up to 100% pore saturation with water vapor. Graphite membranes with controlled porosity can be used as a quantum gate.

The ability to control electronic properties of a material by externally applied fields is at the heart of modern electronics. In many cases, it is the electric field effect that allows one to vary the carrier concentration in a semiconductor device and, consequently, change an electric current through it. In the

<sup>1</sup>Department of Physics, University of Manchester, Oxford Road, Manchester M13 9PL, United Kingdom  
<sup>2</sup>Department of Physics, University of Cambridge, Cavendish Laboratory, Madingley Road, Cambridge CB3 0HJ, United Kingdom

**REPORTS**

**Fig. 5. Conductance modulation (CM)** to show the field-effect on the  $g_{\text{min}}$  (green) and  $g_{\text{max}}$  (red) of the signal (blue) in the  $\mu\text{C}$  gate of the device. The inset shows the  $g_{\text{min}}$  and  $g_{\text{max}}$  versus the voltage of the  $\mu\text{C}$  gate at constant carrier densities.



**Fig. 6. Time-dependent magnetotransport stability** of the signal and the  $g_{\text{min}}$  and  $g_{\text{max}}$  at  $10^6 \text{ V/m}$  for the  $\mu\text{C}$  gate.

carrier efficiency for the read time is  $\approx 0.2$ , which is one order of magnitude of quantum state transfer from the atoms into the photoconductor (12).

We have realized a quantum gate by controlling the magnetotransport of atomic and

**Electric Field Effect in Atomically Thin Carbon Films**

K. S. Novoselov,<sup>1</sup> A. K. Geim,<sup>1</sup> S. V. Morozov,<sup>2</sup> D. Jiang,<sup>1</sup> Y. Zhang,<sup>1</sup> S. V. Dubonos,<sup>1</sup> I. V. Grigorieva,<sup>1</sup> A. A. Firsiroti<sup>1</sup>

We describe nonmetallic graphitic films, which are a new carbon allotrope that are unambiguously stable under ambient conditions, consisting of atomically thin graphite layers. The films are based on the idea of dimensional reduction of a single atomic sheet of graphite to a single atomic surface by intercalation up to 100% pore saturation with water vapor. Graphite membranes with controlled porosity can be used as a quantum gate.

The ability to control electronic properties of a material by externally applied fields is at the heart of modern electronics. In many cases, it is the electric field effect that allows one to vary the carrier concentration in a semiconductor device and, consequently, change an electric current through it. In the

<sup>1</sup>Department of Physics, University of Manchester, Oxford Road, Manchester M13 9PL, United Kingdom  
<sup>2</sup>Department of Physics, University of Cambridge, Cavendish Laboratory, Madingley Road, Cambridge CB3 0HJ, United Kingdom

**REPORTS**

**Fig. 7. Conductance modulation (CM)** to show the field-effect on the  $g_{\text{min}}$  (green) and  $g_{\text{max}}$  (red) of the signal (blue) in the  $\mu\text{C}$  gate of the device. The inset shows the  $g_{\text{min}}$  and  $g_{\text{max}}$  versus the voltage of the  $\mu\text{C}$  gate at constant carrier densities.



**Fig. 8. Time-dependent magnetotransport stability** of the signal and the  $g_{\text{min}}$  and  $g_{\text{max}}$  at  $10^6 \text{ V/m}$  for the  $\mu\text{C}$  gate.

carrier efficiency for the read time is  $\approx 0.2$ , which is one order of magnitude of quantum state transfer from the atoms into the photoconductor (12).

We have realized a quantum gate by controlling the magnetotransport of atomic and

**Electric Field Effect in Atomically Thin Carbon Films**

K. S. Novoselov,<sup>1</sup> A. K. Geim,<sup>1</sup> S. V. Morozov,<sup>2</sup> D. Jiang,<sup>1</sup> Y. Zhang,<sup>1</sup> S. V. Dubonos,<sup>1</sup> I. V. Grigorieva,<sup>1</sup> A. A. Firsiroti<sup>1</sup>

We describe nonmetallic graphitic films, which are a new carbon allotrope that are unambiguously stable under ambient conditions, consisting of atomically thin graphite layers. The films are based on the idea of dimensional reduction of a single atomic sheet of graphite to a single atomic surface by intercalation up to 100% pore saturation with water vapor. Graphite membranes with controlled porosity can be used as a quantum gate.

The ability to control electronic properties of a material by externally applied fields is at the heart of modern electronics. In many cases, it is the electric field effect that allows one to vary the carrier concentration in a semiconductor device and, consequently, change an electric current through it. In the

<sup>1</sup>Department of Physics, University of Manchester, Oxford Road, Manchester M13 9PL, United Kingdom  
<sup>2</sup>Department of Physics, University of Cambridge, Cavendish Laboratory, Madingley Road, Cambridge CB3 0HJ, United Kingdom

**REPORTS**

**Fig. 9. Conductance modulation (CM)** to show the field-effect on the  $g_{\text{min}}$  (green) and  $g_{\text{max}}$  (red) of the signal (blue) in the  $\mu\text{C}$  gate of the device. The inset shows the  $g_{\text{min}}$  and  $g_{\text{max}}$  versus the voltage of the  $\mu\text{C}$  gate at constant carrier densities.



**Fig. 10. Time-dependent magnetotransport stability** of the signal and the  $g_{\text{min}}$  and  $g_{\text{max}}$  at  $10^6 \text{ V/m}$  for the  $\mu\text{C}$  gate.

carrier efficiency for the read time is  $\approx 0.2$ , which is one order of magnitude of quantum state transfer from the atoms into the photoconductor (12).

We have realized a quantum gate by controlling the magnetotransport of atomic and

**Electric Field Effect in Atomically Thin Carbon Films**

K. S. Novoselov,<sup>1</sup> A. K. Geim,<sup>1</sup> S. V. Morozov,<sup>2</sup> D. Jiang,<sup>1</sup> Y. Zhang,<sup>1</sup> S. V. Dubonos,<sup>1</sup> I. V. Grigorieva,<sup>1</sup> A. A. Firsiroti<sup>1</sup>

We describe nonmetallic graphitic films, which are a new carbon allotrope that are unambiguously stable under ambient conditions, consisting of atomically thin graphite layers. The films are based on the idea of dimensional reduction of a single atomic sheet of graphite to a single atomic surface by intercalation up to 100% pore saturation with water vapor. Graphite membranes with controlled porosity can be used as a quantum gate.

The ability to control electronic properties of a material by externally applied fields is at the heart of modern electronics. In many cases, it is the electric field effect that allows one to vary the carrier concentration in a semiconductor device and, consequently, change an electric current through it. In the

<sup>1</sup>Department of Physics, University of Manchester, Oxford Road, Manchester M13 9PL, United Kingdom  
<sup>2</sup>Department of Physics, University of Cambridge, Cavendish Laboratory, Madingley Road, Cambridge CB3 0HJ, United Kingdom

THE ARTICLE  
 Electric Field Effect in Atomically Thin Carbon Films,  
 K. S. Novoselov, et al., Science 306, 666 (2004)



GRAPHENE

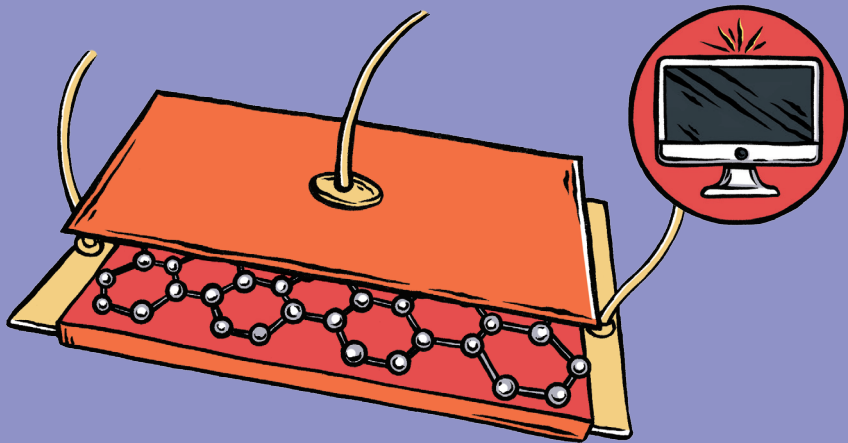


A. GEIM, K. NOVOSELOV, NOBEL PRIZE, 2010

For groundbreaking experiments regarding the two-dimensional material graphene.



GRAPHENE



## NOWADAYS

Graphene could have many applications, especially in nanophysics.  
Perhaps it will play a major role in electronics in the future.



GRAPHENE



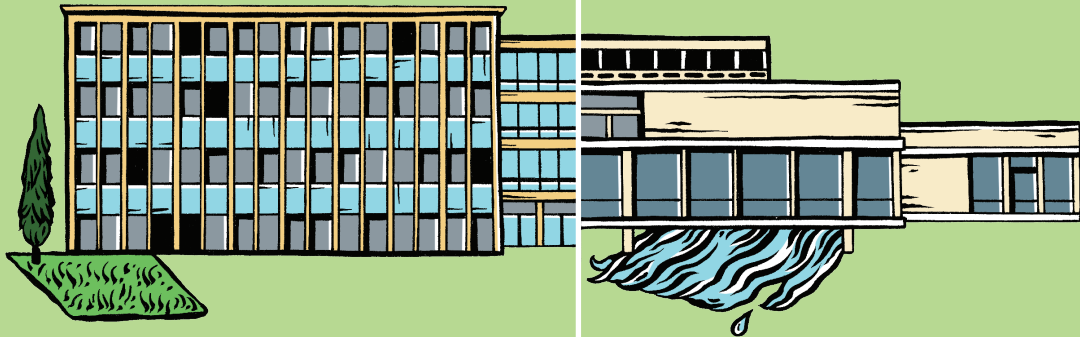


# GIANT MAGNETORESISTANCE

— 1988 —



# GIANT MAGNETORESISTANCE



LABORATOIRE DE PHYSIQUE  
DES SOLIDES, ORSAY, FRANCE

JÜLICH INSTITUTE,  
GERMANY



# GIANT MAGNETORESISTANCE



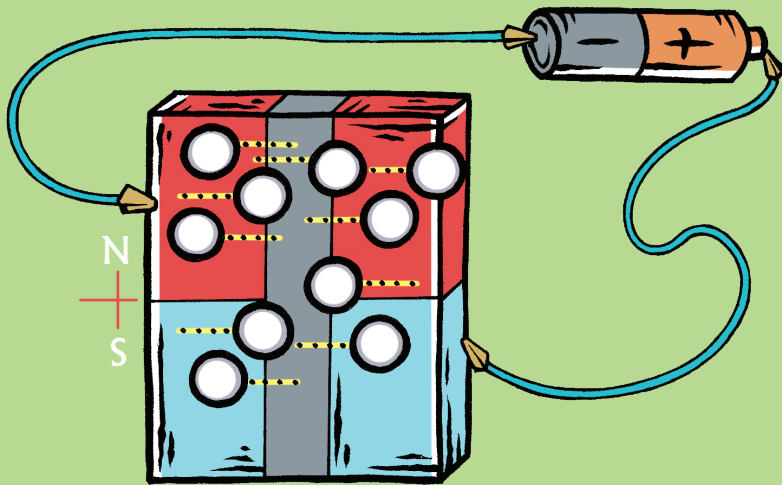
A. FERT



P. GRÜNBERG



# GIANT MAGNETORESISTANCE



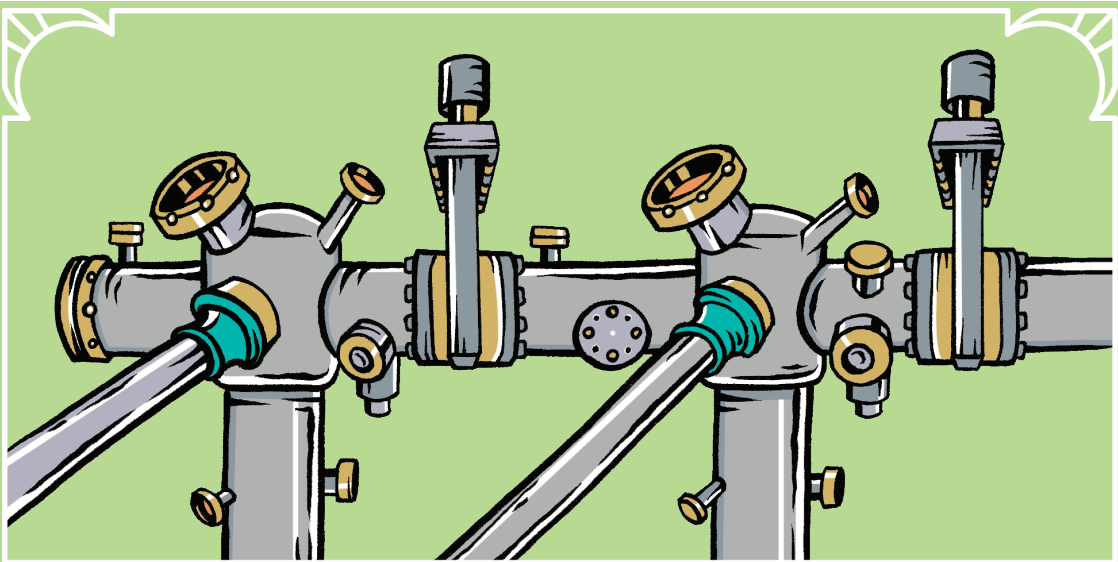
## THE QUESTION

Is electrical current affected by the pole directions in thin magnetic layers ?



# GIANT MAGNETORESISTANCE

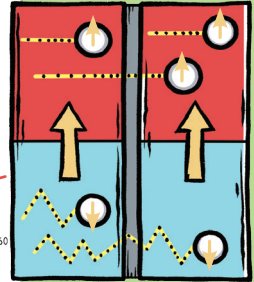
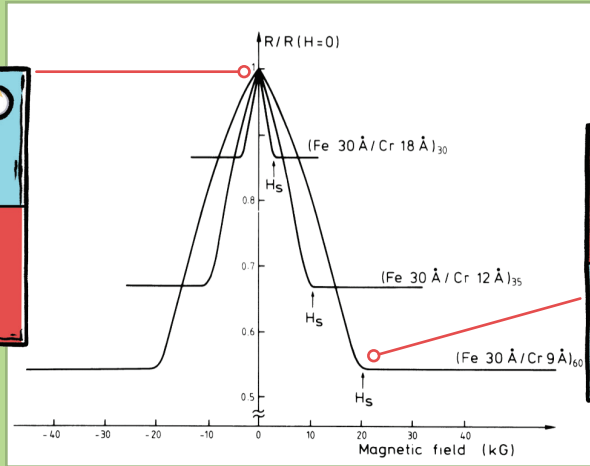
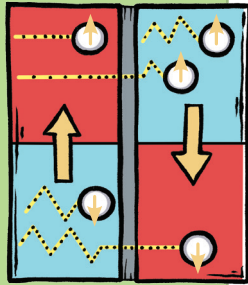




THE LAB



# GIANT MAGNETORESISTANCE



## THE RESULT

If one builds a magnetic “sandwich” and changes its poles, the electrical resistance changes a lot. In fact, the electrons carry a small magnet, the spin, which interacts with the magnetic sandwich.



# GIANT MAGNETORESISTANCE

and the magnetoresistance is lowered when the Cr (FeCo) spacer and Fe (ferromagnetic) layers are alternated.

Giant Magnetoresistance of  $(FeO)_m/(MnO)_n$  Magnetic Superlattices

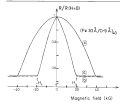


FIG. 2. Magnetoresistance of  $(FeO)_m/(MnO)_n$  superlattices of 2 Å. The current is along [110] and the field is in the layer plane along the current direction.  $\mu_0 H_0$  is the applied field perpendicular to the current direction in the layer plane.  $\mu_0 H_0 \sin \theta$  is the magnetic field in the plane of the superlattice. The numbers in parentheses in Fig. 2 are  $m$ . There is a small difference in the spacer thickness and increasing field. The results are shown in Fig. 2.  $\mu_0 H_0 \sin \theta$  is the magnetic field in the plane of the superlattice. The numbers in parentheses in Fig. 2 are  $m$ .

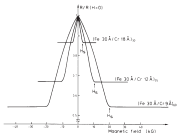


FIG. 3. Magnetoresistance of  $(FeO)_m/(MnO)_n$  superlattices of 2 Å. The current and the applied field are along the same [110] axis as in the case of Fig. 2.

There is no direct comparison of the magnetoresistance of  $(FeO)_m/(MnO)_n$  superlattices with that of  $(FeO)_m/(CoO)_n$  superlattices. However, the magnetoresistance of  $(FeO)_m/(MnO)_n$  superlattices is larger than that of  $(FeO)_m/(CoO)_n$  superlattices. The magnetoresistance of  $(FeO)_m/(MnO)_n$  superlattices is larger than that of  $(FeO)_m/(CoO)_n$  superlattices. The magnetoresistance of  $(FeO)_m/(MnO)_n$  superlattices is larger than that of  $(FeO)_m/(CoO)_n$  superlattices.

of Goring et al.<sup>12</sup> and by the spin-polarized low-temperature magnetoresistance measurements of Carlson and Alvarado.<sup>13</sup> The spin-splitting between the Fe  $d$  states has been studied to indicate correlation between the Cr layers, but a theoretical model for the magnetoresistance is still lacking.<sup>12</sup>

The magnetoresistance of the  $(FeO)_m/(MnO)_n$  superlattices has been studied by a classical technique on small rectangular samples. Examples of magnetoresistance curves at 4.2 K are shown in Fig. 2 and 3. The resistance decreases during the magnetization process and becomes practically constant when the magnetization is saturated. The curves are as in Fig. 2 one obtained for applied fields in the plane of layers in the longitudinal and transverse direction, respectively. The field  $H_0$  is the field parallel to the direction of the current and the current is along the [110] direction.

The most remarkable result exhibited in Fig. 2 and 3 is the large change in the magnetoresistance. The  $\mu_0 H_0 \sin \theta$  is the magnetic field in the plane of the superlattice, and the  $\mu_0 H_0$  is the applied field perpendicular to the current direction in the layer plane.

The most remarkable result exhibited in Fig. 2 and 3 is the large change in the magnetoresistance. The  $\mu_0 H_0 \sin \theta$  is the magnetic field in the plane of the superlattice, and the  $\mu_0 H_0$  is the applied field perpendicular to the current direction in the layer plane.

The most remarkable result exhibited in Fig. 2 and 3 is the large change in the magnetoresistance. The  $\mu_0 H_0 \sin \theta$  is the magnetic field in the plane of the superlattice, and the  $\mu_0 H_0$  is the applied field perpendicular to the current direction in the layer plane.

The most remarkable result exhibited in Fig. 2 and 3 is the large change in the magnetoresistance. The  $\mu_0 H_0 \sin \theta$  is the magnetic field in the plane of the superlattice, and the  $\mu_0 H_0$  is the applied field perpendicular to the current direction in the layer plane.

Enhanced magnetoresistance in layered magnetic structures with antiferromagnetic interface exchange

Enhanced magnetoresistance in layered magnetic structures with antiferromagnetic interface exchange

G. Binasch, F. Grünberg, F. Saurebich, and W. Zinn

*Institut für Hochenergiephysik, Kernforschungsanlage Jülich 4 in A. Postfach 1913, D-5170 Jülich, West Germany*

(Received 11 May 1988; revised received 12 December 1988)

Enhanced magnetoresistance in layered magnetic structures with antiferromagnetic interface exchange

G. Binasch, F. Grünberg, F. Saurebich, and W. Zinn

*Institut für Hochenergiephysik, Kernforschungsanlage Jülich 4 in A. Postfach 1913, D-5170 Jülich, West Germany*

(Received 11 May 1988; revised received 12 December 1988)

The orbital moments of  $(FeO)_m/(MnO)_n$  layers with antiferromagnetic interface exchange increase when the magnetization of the Fe layers is aligned antiparallel. The effect is much stronger than the usual anisotropic magnetoresistance and further increases in structures with more than two layers. It can be explained in terms of spin-dependent scattering of conduction electrons caused by the spin-orbit coupling of the magnetization.

Recently there is much interest in layered magnetic structures, which is partly due to the prospect that layer-by-layer properties, such as the electrical conductivity or the optical absorption, can be used to modify the material properties or to obtain new properties, such as optoelectronic devices. In the past few years we have concentrated our research on the preparation of the epitaxially growing ferromagnetic layers with an antiferromagnetic interface. In layered magnetic structures with antiferromagnetic interface exchange the spin-orbit coupling of the magnetization of the most simple structure when this question can be investigated, i.e., a magnetic double layer consisting of two ferromagnetic films separated by a film of another material. A very interesting case which is treated during this paper is the spin-orbit coupling of the magnetization of Cr as sketched in Fig. 1. In these films one of naturally good nonmagnetic conductors and of the thickness of the Cr film is approximately 1 nm, then we observed that the effective exchange coupling of the Fe layers across the Cr is well-defined (AF). This happens for arbitrary geometry of the layered  $(FeO)_m/(MnO)_n$  structure both along the [110] and [111] directions.

Although the microscopic origin of this AF coupling up to now remains speculative, we found that such structures display some novel and unique magnetic properties both in their static and dynamic behavior.<sup>1</sup> The new features we report on here and which also occur as a result of the AF coupling in a strong extension of the spin-orbit coupling effect. Using magnetoresistance measurements the unusual anisotropic effect, i.e., the difference in magnetoresistance between the longitudinal and the transverse ( $\mu_0 H \perp I$ ) to the magnetization. As it has been shown in layered structures with AF coupling a change in resistivity due to antiparallel alignment of the magnetizations in the ferromagnetic films can be observed. In this effect, it is shown that this is an anisotropic aspect for spin-orbit coupling.<sup>2</sup>

We have two methods available to magnetize AF coupling, namely ferromagnetic current perpendicular to the magnetization and light scattering (LS) from spin waves. A more accurate description has been given elsewhere.<sup>3</sup> Here we will explain the microscopic origin of the effect. The effect is much stronger than the usual anisotropic magnetoresistance and further increases in structures with more than two layers. It can be explained in terms of spin-dependent scattering of conduction electrons caused by the spin-orbit coupling of the magnetization.

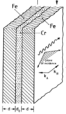


FIG. 1. Ferromagnetic double layer with antiparallel alignment of the magnetizations. Also indicated is the spin of the conduction electrons which is antiparallel to the light scattering direction and further across the MnO<sub>n</sub> film.

Enhanced magnetoresistance in layered magnetic structures with antiferromagnetic interface exchange

Enhanced magnetoresistance in layered magnetic structures with antiferromagnetic interface exchange

G. Binasch, F. Grünberg, F. Saurebich, and W. Zinn

*Institut für Hochenergiephysik, Kernforschungsanlage Jülich 4 in A. Postfach 1913, D-5170 Jülich, West Germany*

(Received 11 May 1988; revised received 12 December 1988)

The orbital moments of  $(FeO)_m/(MnO)_n$  layers with antiferromagnetic interface exchange increase when the magnetization of the Fe layers is aligned antiparallel. The effect is much stronger than the usual anisotropic magnetoresistance and further increases in structures with more than two layers. It can be explained in terms of spin-dependent scattering of conduction electrons caused by the spin-orbit coupling of the magnetization.

Recently there is much interest in layered magnetic structures, which is partly due to the prospect that layer-by-layer properties, such as the electrical conductivity or the optical absorption, can be used to modify the material properties or to obtain new properties, such as optoelectronic devices. In the past few years we have concentrated our research on the preparation of the epitaxially growing ferromagnetic layers with an antiferromagnetic interface. In layered magnetic structures with antiferromagnetic interface exchange the spin-orbit coupling of the magnetization of the most simple structure when this question can be investigated, i.e., a magnetic double layer consisting of two ferromagnetic films separated by a film of another material. A very interesting case which is treated during this paper is the spin-orbit coupling of the magnetization of Cr as sketched in Fig. 1. In these films one of naturally good nonmagnetic conductors and of the thickness of the Cr film is approximately 1 nm, then we observed that the effective exchange coupling of the Fe layers across the Cr is well-defined (AF). This happens for arbitrary geometry of the layered  $(FeO)_m/(MnO)_n$  structure both along the [110] and [111] directions.

Although the microscopic origin of this AF coupling up to now remains speculative, we found that such structures display some novel and unique magnetic properties both in their static and dynamic behavior.<sup>1</sup> The new features we report on here and which also occur as a result of the AF coupling in a strong extension of the spin-orbit coupling effect. Using magnetoresistance measurements the unusual anisotropic effect, i.e., the difference in magnetoresistance between the longitudinal and the transverse ( $\mu_0 H \perp I$ ) to the magnetization. As it has been shown in layered structures with AF coupling a change in resistivity due to antiparallel alignment of the magnetizations in the ferromagnetic films can be observed. In this effect, it is shown that this is an anisotropic aspect for spin-orbit coupling.<sup>2</sup>

We have two methods available to magnetize AF coupling, namely ferromagnetic current perpendicular to the magnetization and light scattering (LS) from spin waves. A more accurate description has been given elsewhere.<sup>3</sup> Here we will explain the microscopic origin of the effect. The effect is much stronger than the usual anisotropic magnetoresistance and further increases in structures with more than two layers. It can be explained in terms of spin-dependent scattering of conduction electrons caused by the spin-orbit coupling of the magnetization.

THE ARTICLES  
Giant magnetoresistance of Cr magnetic superlattices, M. N. Baibich et al., PRL 61, 2472 (1988)  
Enhanced magnetoresistance in layered magnetic structures, G. Binasch et al., PRB, 39, 4828 (1989)



# GIANT MAGNETORESISTANCE



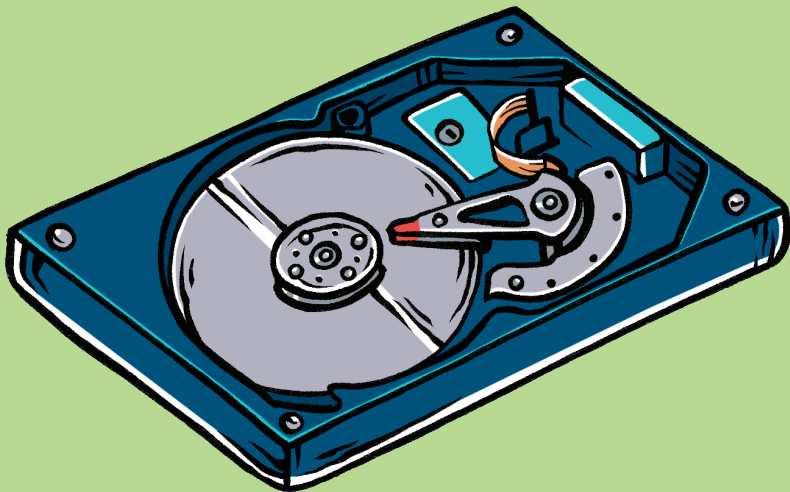
A. FERT, P. GRÜNBERG, NOBEL PRIZE, 2007

For the discovery of giant magnetoresistance.



# GIANT MAGNETORESISTANCE





## NOWADAYS

This discovery allowed to develop the read-out head for hard disks.  
It has also opened a new field of research called spintronics.



# GIANT MAGNETORESISTANCE



# SUPERCONDUCTIVITY

— 1911 —



# SUPERCONDUCTIVITY



LEYDEN UNIVERSITY, NETHERLANDS



# SUPERCONDUCTIVITY

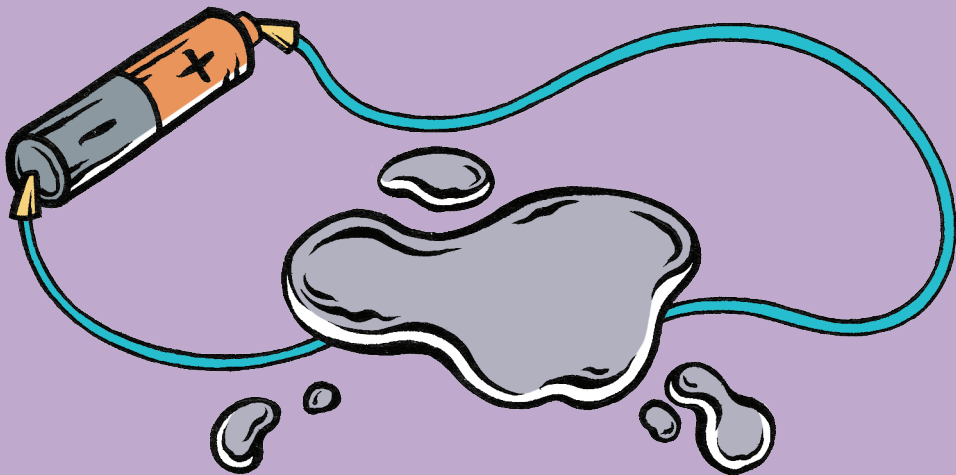


K. ONNES



# SUPERCONDUCTIVITY



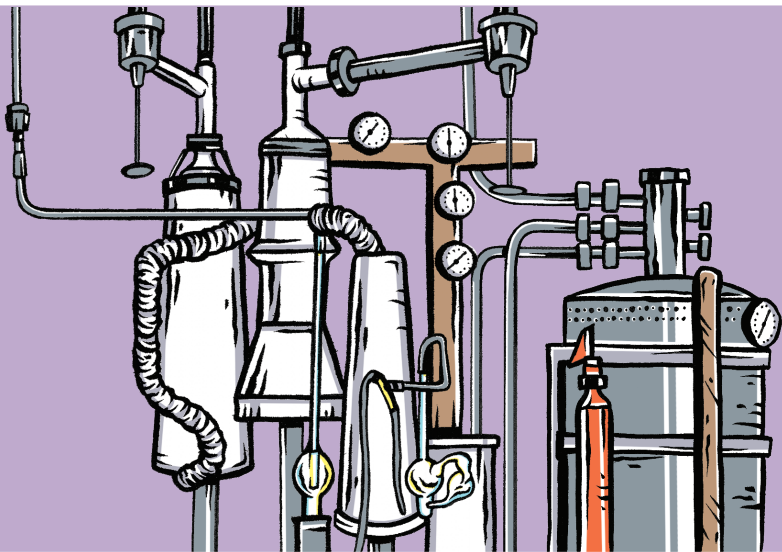


## THE QUESTION

Does a metal such as mercury conduct better or worse at low temperature?



# SUPERCONDUCTIVITY

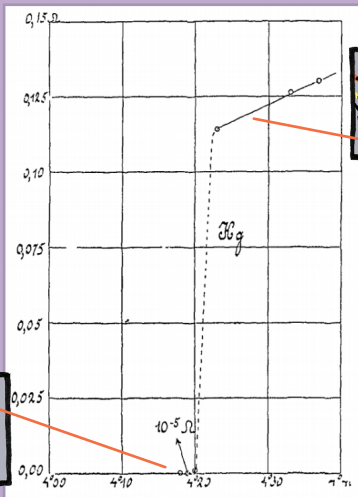
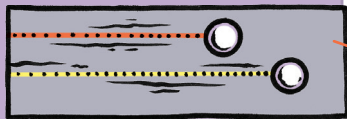


## THE LAB

Onnes uses liquid helium to cool down the metal at a few degrees above absolute zero.



# SUPERCONDUCTIVITY



## THE RESULT

The electrical resistance of mercury suddenly drops down to zero at low temperatures.  
The metal conducts perfectly: this is superconductivity.



# SUPERCONDUCTIVITY

decide, a theory of course which first of all takes account of the fundamental chemical facts which we mentioned above, but which further succeeds in avoiding the drawbacks — particularly with respect to the specific heats — which adhere to the hypothesis on the chemical forces hatched more at length in our previous paper. And then it cannot be doubtful, in our opinion, by what way we shall have to try to find such a theory. We shall have to extend the theory of indivisible units of energy, which has led to such remarkable results, to the chemical phenomena; it will be necessary to investigate in what way the properties of the reversible chemical reactions are connected with the phenomena of radiation. When this connection has been found, the course is indicated to calculate the difference of entropy of a chemical reaction by the aid of the statistical theory of entropy at temperatures at which this reaction can actually take place, and then it will be very simple to calculate by the aid of the acquired knowledge of the specific heats the difference of entropy also for temperatures, at which there can no longer be question of chemical reactions.

One of us has been occupied with this question, and hopes to be able before very long to publish further communications on this subject.

**Physics.** — "Further Experiments with Liquid Helium. G. On the Electrical Resistance of Pure Metals, etc. VI. On the Sudden Change in the Rate at which the Resistance of Mercury Disappears." By H. KAMERLINGH ONNES. Communication N° 124c from the Physical Laboratory at Leyden.

(Communicated in the meeting of November 25, 1911.)

§ 1. *Introduction.* In Comm. N° 123b (Proc. May 1911) I mentioned that just before this resistance disappeared practically altogether, its rate of diminution with falling temperature became much greater than that given by the formula of Comm. N° 119. In the present paper a closer investigation is made of this phenomenon.

§ 2. *Arrangement of the resistance.* A description was given in Comm. N° 123 (Proc. June 1911) of the cryostat which, by allowing the contained liquid to be stirred, enabled me to keep resistances at uniform well-defined temperatures; and in that paper I also mentioned that measurements of the resistance of mercury at the lowest possible temperatures had been repeated using a mercury resistance with mercury leads. The immersion of a resistance with such leads in a bath of liquid helium was rendered possible only by the successful construction of that cryostat.

The accompanying Plate, which should be compared with the Plate of Comm. N° 123, shows the mercury resistance with a portion of the leads; it is represented diagrammatically in fig. 1. Seven glass U-tubes of about 0.005 sq. mm. cross section are joined together at their upper ends by inverted Y-pieces which are sealed off above, and are not quite filled with mercury; this gives the mercury an opportunity to contract or expand on freezing or liquefying without breaking the glass and without breaking the continuity of the mercury thread formed in the seven U-tubes. To the Y-pieces  $b_1$  and  $b_2$  are attached two leading tubes  $Hg_{11}$ ,  $Hg_{12}$ , and  $Hg_{21}$ ,  $Hg_{22}$  (whose lower portions are shown at  $Hg'_{11}$ ,  $Hg'_{12}$ ,  $Hg'_{21}$ ,  $Hg'_{22}$ ) filled with mercury which, on solidification, forms four leads of solid mercury. To the connector  $b_3$  is attached a single tube  $Hg_3$ , whose lower part is shown at  $Hg'_3$ . At  $b_4$  and  $b_5$  current enters and leaves through the tubes  $Hg_4$  and  $Hg_5$ ; the tubes  $Hg_4$  and  $Hg_5$  can be used for the same purpose or also for determining the potential difference between the ends of the mercury thread. The mercury filled tube  $Hg_6$  can be used for measuring the potential at the point  $b_6$ . To take up less space in the cryostat and to find room alongside the stirring pump  $S$ , the tubes which are shown in one plane in fig. 1 were closed together in the manner shown in fig. 2. The position in the cryostat is to be seen from fig. 4 where the other parts are indicated by the same letters as were used in the Plate of Comm. N° 123. The leads project above the cover  $S$ , in a manner shown in perspective in fig. 3. They too are provided with expansion spaces, while in the bent side pieces are fused platinum wires  $Hg'_1$ ,  $Hg'_2$ ,  $Hg'_3$ ,  $Hg'_4$ ,  $Hg'_5$ , which are connected to the measuring apparatus. The apparatus was filled with mercury distilled over in vacuo at a temperature of 60° to 70° C. while the cold portion of the distilling apparatus was immersed in liquid air.

§ 3. *Results of the Measurements.* The junctions of the platinum wires with the copper leads of the measuring apparatus were protected as effectively as possible from temperature variation. The mercury resistance itself with the mercury leads, which served for the measurement of the fall of potential assumed, however, an immersion in liquid helium to be the seat of a considerable thermo-electric force in spite of the care taken to fill it with perfectly pure mercury. The magnitude of this thermo-electric effect did not change much when the resistance was immersed in liquid hydrogen or in liquid air instead of in liquid helium, and we may therefore conclude that it is intimately connected with phenomena which occur in the neigh-

H. KAMERLINGH ONNES. "Further Experiments with Liquid Helium. F. Isotherms of Monoclinic Glass, etc. IX. Thermal Properties of Helium."

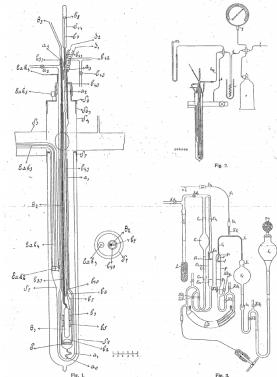


Fig. 1.   
 *Verduidelijde Liquid Anal. Amsterdam, Vol. XIV.*

## THE ARTICLE

Further experiments with Liquid Helium  
Com. N°124c from the Phys. Lab. at Leyden, 1911



# SUPERCONDUCTIVITY





## K.ONNES, NOBEL PRIZE, 1913

For his investigations on the properties of matter at low temperatures which led, inter alia, to the production of liquid helium.



# SUPERCONDUCTIVITY



## NOWADAYS

levitating train: the fastest in the world; medical resonance imaging (MRI);  
electrical cables: for a better electrical conduction



# SUPERCONDUCTIVITY

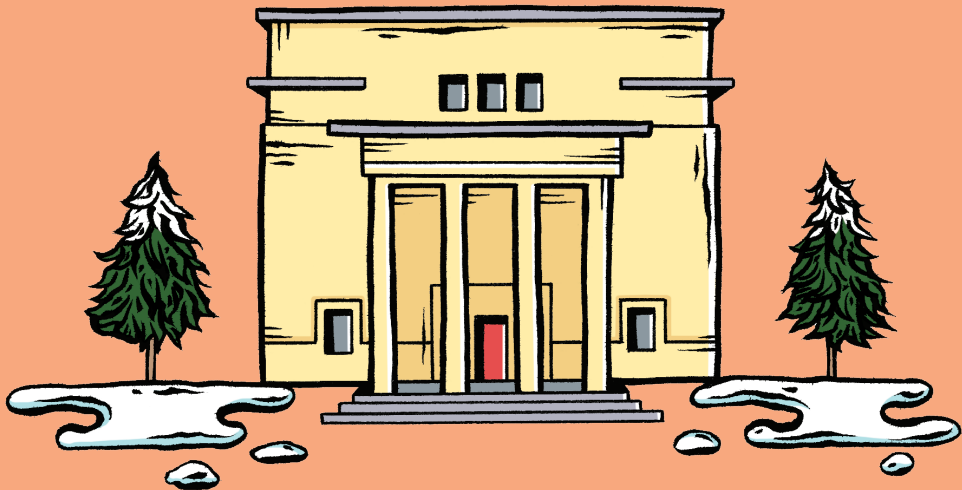


# SUPERFLUIDITY

— 1937 —



# SUPERFLUIDITY



INSTITUTE FOR PHYSICAL PROBLEMS,  
MOSCOW, RUSSIA



# SUPERFLUIDITY

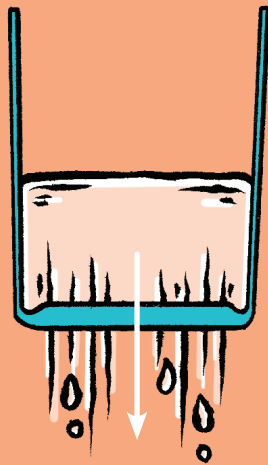




P. KAPITSA



# SUPERFLUIDITY

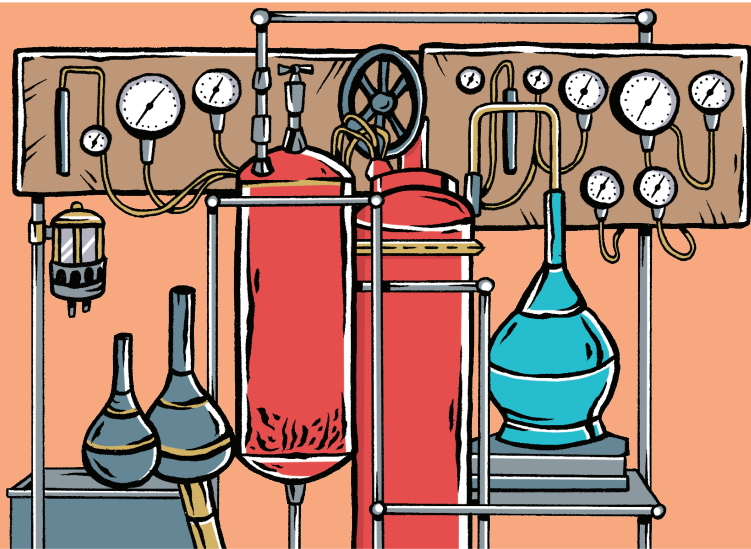


## THE QUESTION

What does a liquid become close to absolute zero if it doesn't freeze?



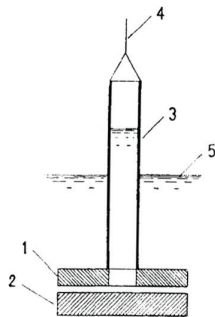
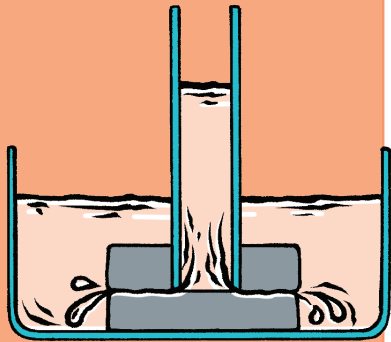
# SUPERFLUIDITY



THE LAB



# SUPERFLUIDITY



The very small kinematic viscosity of liquid helium II thus makes it difficult to measure the viscosity. In an attempt to get laminar motion the following method (shown diagrammatically in the accompanying illustration) was devised. The viscosity was measured by the pressure drop when the liquid flows through the gap between the disks 1 and 2; these disks were of glass and were optically

flat, the gap between them being adjustable by mica distance pieces. The upper disk, 1, was 3 cm. in diameter with a central hole of 1.5 cm. diameter, over which a glass tube (3) was fixed. Lowering and raising this plunger in the liquid helium by means of the thread (4), the level of the liquid column in the

## THE RESULT

Helium is placed in a column above two disks close to absolute zero. It succeeds to flow between the disks even when they touch each other. Kapitsa calls it superfluidity.



# SUPERFLUIDITY



Letters to the Editor

The Editor then will hold himself responsible for criticism regarding his responsibility. His present undertakings in nature, or as compared with the nature of signed manuscripts intended for this or any other part of NATURE. No notice or notice of acceptance communication.

NOTES ON PAGES IN SOME OF THIS WEEK'S LETTERS APPEAR ON P. 82.

COMMUNICATIONS ARE INVITED TO ATTEND REGULAR MEETINGS TO THEIR CORRESPONDENTS.

Viscosity of Liquid Helium below the  $\lambda$ -Point. This abnormally high heat conductivity of helium... below the  $\lambda$ -point, as first observed by Kapitza... of anomalous character. This phenomenon... viscosity  $\eta$  is to have an abnormally high... at present, the only viscosity measurements... below the  $\lambda$ -point for a liquid with helium... showed that there is a drop in viscosity below... by a factor of 1.5 to 2.0, depending on the... apparatus, however, no check was made to... that the section was laminar, and not the

important fact that liquid helium has a... of viscosity of about 1/10 the one above... of an ordinary fluid, with its viscosity... only comparable to that of a gas, neither... viscosity is 1/10 comparable only... very high, which is in order to keep the section... especially in the normal state in Yermakov... the lowering of an oscillating cylinder, the... number must be kept very low. This... was not fulfilled in the Yermakov experi... the desired range of viscosity thus refer... and consequently may not be satisfactorily... than the real value.

The very small laminar conductivity of liquid helium... present state than that of hydrogen gas... through to be the best of the... The present liquid is perhaps sufficient to require... working with superconducting, since the liquid... the  $\lambda$ -point occurs a special case which could be... do so far below... viscosity may be indicated by our experiments... (1937), and for the other maximum viscosity... condition that the turbulent motion, however it... in the turbulent region, is not... with the liquid helium. It might be assumed of the... that the thermal conductivity was... would be sufficient to explain the... almost exclusively by Kapitza.

By J. F. ALLEN, A. D. MISENER, and J. G. KAPITSA, Institute of Physical Problems, Moscow. Received Jan. 5, 1938. (This paper was received at the Editor's office, White, Moscow on Dec. 21, 1937.)



Flow of Liquid Helium II

A survey of the various properties of liquid helium II has presented us in an attempt to viscosity... that of our fluid experimentally... an upper limit of  $10^{-7}$  c.g.s. units for the viscosity... II is assuming the character of an oscillating cylinder. We had reached the same conclusion as Kapitza in... the high Reynolds number in... velocity, the measurements probably... special case because flow.

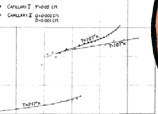
The present data were obtained from observations on the flow of liquid helium II through capillary tubes. The capillaries were made of Pyrex glass, with diameters from 0.005 to 0.010 cm. and lengths 1.00 cm. and 1.50 cm. The flow was measured by a manometer with a diameter of 2.0 cm. and an oil level of diluted bromine with an average of 1.00 cm. and 0.002 cm., which was attached to a manometer of 1.00 cm. diameter. The measurements were made by raising or lowering the reservoir with an attached capillary so that the level of liquid helium in the reservoir was a centimetre or so above or below that of the surrounding liquid helium bath. The rate of change of level in the reservoir was then determined from the continuous eye piece scale and a stop-watch; measurements were made until the levels became constant. The data showing relations of flow through the capillary and the corresponding pressure differences at the ends of the capillary are given in the accompanying table and plotted on a logarithmic scale in the diagram.

TABLE I. Flow of liquid helium II through capillary tubes. The values of  $\eta$  are calculated from the data in the table.

Table with 4 columns: Tube No., P (cm Hg), F (cm^3/sec), and η (c.g.s. units). Rows 1-10 show data for different tubes and pressures.

The following facts are evident: (1) The viscosity of flow, for given pressure level and given temperature, changes by about a factor of 10 with a change of temperature from 1.0° K. to 2.0° K. (2) With the larger capillary and slightly higher velocities of flow, the pressure-viscosity relation is approximately  $\eta \propto P^2$ , with the power of  $\eta$  decreasing as the velocity is increased.

If, for the purpose of calculating a possible upper limit to the viscosity, we assume the critical flow velocity, that is,  $\eta \approx 10^{-7}$  c.g.s. units, we obtain the value  $\eta \approx 10^{-7}$  c.g.s. units, which is... upper limit given by Kapitza who, using velocities of the order of magnitude higher than ours, had obtained



the relation  $\eta \propto P^2$  and an upper limit to the viscosity of  $\eta \approx 10^{-7}$  c.g.s. units. The observed type of flow, however, in which the velocity becomes almost independent of pressure, most certainly cannot be limited as laminar or even an ordinary turbulent flow. Consequently any known pressure differences, from our data, are of the order of magnitude which would have been assumed. It is not possible that the liquid helium II also over the limits of the table. In this case our data would be incapable of showing the 'laminar' flow of the liquid.

With regard to the suggestion that the high thermal conductivity of helium II might be explained by turbulence, we have calculated that the flow velocity necessary to transport all the heat input over the observed temperature gradient in the Allen, Pridmore and Gable experiment is about 100 cm/sec. On the other hand, the greatest flow velocity produced by oscillation and by the pressure difference along the vertical section capillary will not be likely to be greater than 10 cm/sec. It seems, therefore, that turbulent turbulent motion cannot account for an appreciable part of the high thermal conductivity which has been observed for helium II.

A. D. MISENER, Institute of Physical Problems, Moscow. Received Jan. 5, 1938. (This paper was received at the Editor's office, White, Moscow on Dec. 21, 1937.)

Some Experiments on Radio Frequency Superconductivity. Measurements were made on an extended tin wire carrying an alternating current of a frequency of about 100 kilocycles per second supported in a direct current. The resulting magnetic field at the surface of the wire was then measured to points electrolytically.



THE ARTICLES

Viscosity of Liquid Helium below the  $\lambda$ -Point, P. Kapitza, Nature 74, 141 (1938)
Flow of liquid helium II, J.F. Allen, A.D. Misener, Nature 75, 141 (1938)



# SUPERFLUIDITY

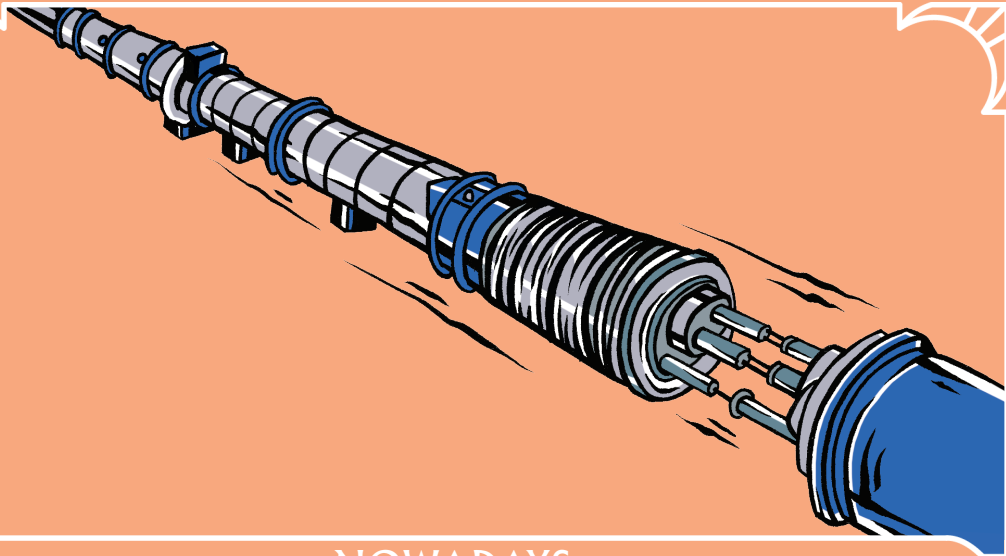


## P. KAPITSA, NOBEL PRIZE, 1978

For his basic inventions and discoveries in the area of low-temperature physics.



# SUPERFLUIDITY



## NOWADAYS

Superfluid helium allows to cool down particle accelerators such as LHC.  
It is also an essential tool for physics research close to absolute zero.



# SUPERFLUIDITY

The image features a teal background with a white decorative border. The border consists of a thin white line that forms a rectangular frame. At each of the four corners, the border turns inward, creating a quarter-circle arc. Inside each of these arcs, there are several short, parallel white lines radiating from the center of the arc towards the corners, giving the impression of a stylized corner ornament or a decorative flourish.

TOPOLOGY  
– 1972 – 1985 –

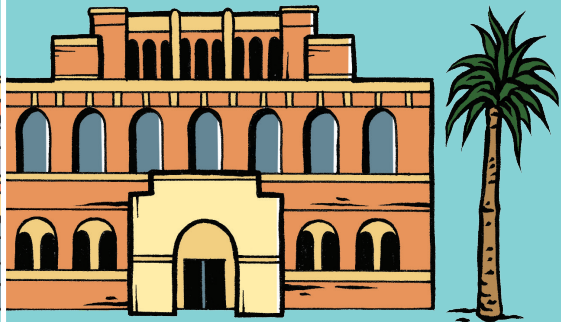


# TOPOLOGY





BIRMINGHAM UNIVERSITY,  
GREAT BRITAIN



UNIVERSITY OF SOUTHERN  
CALIFORNIA, USA

The image features a solid teal background. A white decorative border frames the central area, with ornate, curved corner pieces at each of the four corners. The word "TOPOLOGY" is centered in the middle of the page in a white, serif, all-caps font.

# TOPOLOGY



D. THOULESS



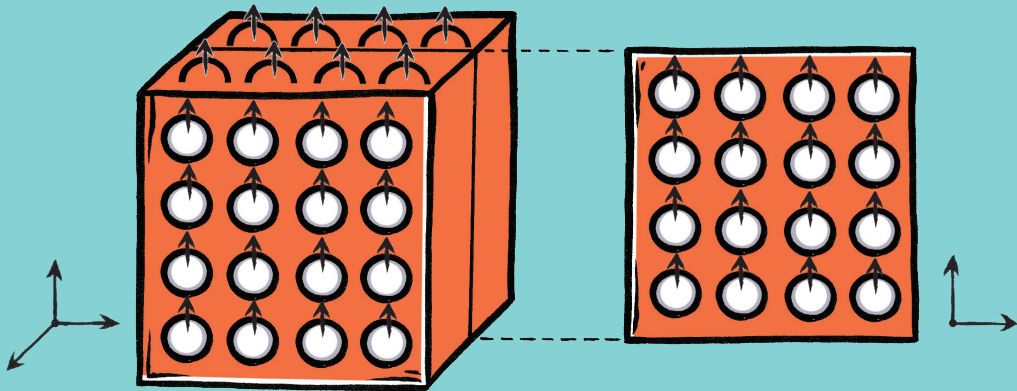
M. KOSTERLITZ



D. HALDANE

The image features a solid teal background. A white decorative border frames the entire area, with ornate, curved corner pieces at each of the four corners. In the center of the teal field, the word "TOPOLOGY" is written in a white, all-caps, serif font.

# TOPOLOGY

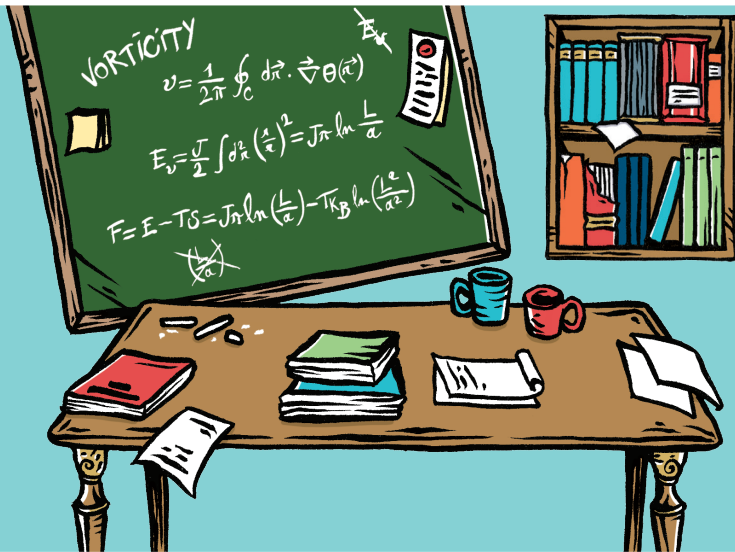


## THE QUESTION

Can a superconductor or a magnet exist in two dimensions?

The image features a solid teal background. A white decorative border frames the entire area, with ornate, curved corner pieces at each of the four corners. In the center of the teal field, the word "TOPOLOGY" is written in a white, all-caps, serif font.

# TOPOLOGY



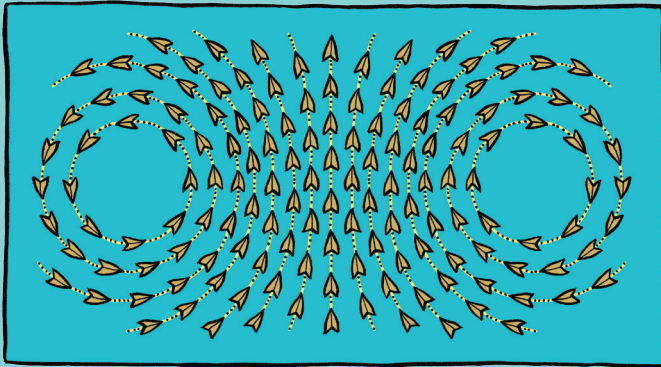
THE LAB

The image features a solid teal background. A white decorative border frames the central area, with ornate, curved corner pieces at each of the four corners. The word "TOPOLOGY" is centered in the middle of the page in a white, serif, all-caps font.

# TOPOLOGY



$$\frac{\pi J}{k_B T_c} - 1 \approx \pi \tilde{y}_c(0) \exp\left(\frac{-\pi^2 J}{k_B T_c}\right) \approx 0.12.$$



## THE RESULT

New states can appear in solids for topological reasons. For example in magnets or 2D superfluids, vortex and anti-vortex appear which allow the order to survive.

The image features a solid teal background. A white decorative border frames the central area, with ornate, curved corner pieces at each of the four corners. The word "TOPOLOGY" is centered in the middle of the page in a white, all-caps, serif font.

# TOPOLOGY

**Ordering, metastability and phase transitions in two-dimensional systems**

J.M. Kosterlitz and D.J. Thouless  
Department of Mathematical Physics, University of Birmingham, Birmingham B15 2TT, U.K.

Received 12 November 1972

*Abstract.* A new definition of order called topological order is proposed for two-dimensional systems in which no long-range order of the conventional type exists. The possibility of a phase transition characterized by a change in the response of the system to an external perturbation is discussed in the context of a mean field type of approximation. The critical behaviour found in this model displays very weak singularities. The appearance of these lines in the  $xy$  model of magnetism, the vortex liquid transition, and the vortex superfluid are discussed. This type of phase transition cannot occur in a representative set in a Heisenberg ferromagnet for reasons that are given.

**1. Introduction**

Pearls (1955) has argued that thermal motion of long-wavelength phonons will destroy the long-range order of a two-dimensional solid in the sense that the mean square deviation of an atom from its equilibrium position increases logarithmically with the size of the system, and the Bragg peaks of the diffraction pattern formed by the system are broad instead of sharp. The absence of long-range order of this simple form has been shown by Mermin (1969) using rigorous inequalities. Similar arguments can be used to show that there is no spontaneous magnetization in a two-dimensional magnet with spins with more than one degree of freedom (Mermin and Wagner 1966) and that the expectation value of the superfluid order parameter in a two-dimensional Bose fluid is zero (Hohenberg 1967).

On the other hand there is inconclusive evidence from the numerical work on a two-dimensional system of hard discs by Alder and Wainwright (1962) of a phase transition between a gaseous and solid state. Stanley and Kaplan (1966) found that high-temperature series expansions for two-dimensional spin models indicated a phase transition in which the susceptibility becomes infinite. The evidence for such a transition is much stronger for the  $xy$  model (spins confined to a plane) than for the Heisenberg model, as can be seen from the papers of Stanley (1965) and Moore (1969). Low-temperature expansions obtained by Wagner (1967) and Berenzinski (1970) give a magnetization proportional to some power of the field between zero and unity, and indicate the possibility of a sharp transition between such behaviour and the high-temperature regime where the magnetization is proportional to the applied field.

In this paper we present arguments in favour of a quite different definition of long-range order which is based on the overall properties of the system rather than on the

To conclude this section on the model system, we would like to point out that the assumption of a very dilute system ( $e^{-2\mu\phi} \ll 1$ ) is not necessarily valid in a real system. However, we expect that the qualitative arguments will go through even in such a case and the general form of the results will be unchanged. We can imagine increasing the cutoff  $r_0$  to some value  $R_0$  such that the energy of two charges a distance  $R_0$  apart is  $2\mu\phi(R_0)$  where  $\exp(-2\mu\phi(R_0)) \ll 1$ . For charges further apart than  $R_0$ , we can use the theory as outlined previously. The boundary conditions given by equation (20) will be changed to

$$y(0) = \frac{2\mu}{\int_{R_0}^{\infty} \frac{1}{R} dR} - 4 \quad (41)$$

with  $\phi(R_0)$  an unknown function. The critical temperature and the dielectric constant will now be determined in terms of  $\phi(R_0)$  and  $\mu\phi(R_0)$ . To determine these two quantities, a more sophisticated treatment is required, but we expect that the behaviour of the dielectric constant and specific heat at the critical temperature will be unchanged.

**3. The two-dimensional  $xy$  model**

The two-dimensional  $xy$  model is a system of spins constrained to rotate in the plane of the lattice which, for simplicity, we take to be a simple square lattice with spacing  $a$ . The hamiltonian of the system is

$$H = -J \sum_{\langle ij \rangle} \mathbf{S}_i \cdot \mathbf{S}_j = -J \sum_{\langle ij \rangle} \cos(\phi_i - \phi_j) \quad (42)$$

where  $J > 0$  and the sum  $\langle ij \rangle$  over lattice sites is over nearest neighbours only. We have taken  $|\mathbf{S}_i| = 1$  and  $\phi_i$  is the angle the  $i$ th spin makes with some arbitrary axis. Only slowly varying configurations, that is, those with adjacent angles nearly equal, will give any significant contribution to the partition function so that we expand the hamiltonian up to terms quadratic in the angles.

It has been shown by many authors (Mermin and Wagner 1966, Wagner 1967, Berenzinski 1970) that this system does not have any long-range order at the ground state is unstable against low-energy spin-wave excitations. However, there is some evidence (Stanley 1966, Moore 1969) that this system has a phase transition, but it cannot be of the usual type with finite mean magnetization below  $T_c$ . As we shall show, there exist metastable states corresponding to vortices which are closely bound in pairs below some critical temperature, while above this they become free. The transition is characterized by a sudden change in the response to an applied magnetic field.

Expanding about a local minimum of  $H$

$$H - E_0 = \frac{1}{2} J \sum_{\langle ij \rangle} (\phi_i - \phi_j)^2 = J \sum_{\langle ij \rangle} \Delta\phi(r)^2 \quad (43)$$

where  $\Delta$  denotes the first difference operator,  $\phi(r)$  is a function defined over the lattice sites, and the sum is taken over all sites of the lattice. If we consider the system in the configuration of figure 1, its energy is given by equation (43)

$$H - E_0 = \pi J \sum_{\langle ij \rangle} \phi \quad (44)$$

where  $R$  is the radius of the system. Thus we have a slowly varying configuration, which we shall call a vortex, whose energy increases logarithmically with the size of the system.

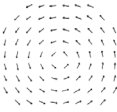


Figure 1. A vortex in the  $xy$  model.

From the arguments of the Introduction, this suggests that a suitable description of the system is to approximate the hamiltonian by terms quadratic in  $\Delta\phi(r)$  and split this up into a term corresponding to the vortices and another to the low-energy excitations (spin waves).

We extend the domain of  $\phi(r)$  to  $-\infty < \phi(r) < \infty$  to allow for the fact that, in the absence of vortices,  $\langle \phi(r) - \phi(r') \rangle$  increases like  $\ln |(r - r')|$  (Berenzinski 1971). Thus, at large separations, the spins will have gone through several revolutions relative to one another. If we now consider a vortex configuration of the type of figure 1, as we go round some closed path containing the centre of the vortex,  $\phi(r)$  will change by  $2\pi$  for each revolution. Thus, for a configuration with no vortices, the function  $\phi(r)$  will be single-valued, while for one with vortices it will be multi-valued. This may be summarized by

$$\oint \Delta\phi(r) = 2\pi q \quad q = 0, \pm 1, \pm 2, \dots \quad (45)$$

where the sum is over some closed contour on the lattice and the number  $q$  defines the total strength of the vortex distribution contained in the contour. If a single vortex of the type shown in figure 1 is contained in the contour, then  $q = 1$ .

Let now  $\phi(r) = \phi_0(r) + \phi(r)$ , where  $\phi_0(r)$  defines the angular distribution of the spins in the configuration of the local minimum, and  $\phi(r)$  the deviation from this. The energy of the system is now

$$H - E_0 = J \sum_{\langle ij \rangle} (\Delta\phi(r))^2 + J \sum_{\langle ij \rangle} \Delta\phi(r)^2 \quad (46)$$

where

$$\sum_{\langle ij \rangle} \Delta\phi(r) = 0 \quad \text{and} \quad \sum_{\langle ij \rangle} \Delta\phi(r) = 2\pi q. \quad (47)$$

The cross term vanishes because of the condition (47) obeyed by  $\phi(r)$ . Clearly the configuration of absolute minimum energy corresponds to  $q = 0$  for every possible contour when  $\Delta\phi(r)$  is the same for all lattice sites. We see from equation (45) that, if we shrink the contour so that it passes through only four sites as in figure 2, we will obtain the strength

**THE ARTICLE**

*Ordering, metastability and phase transitions in two-dimensional systems*

J.M. Kosterlitz, D.J. Thouless, Journal of Physics C: Solid State Physics, 6, 1181 (1973).

The image features a solid teal background. A white decorative border frames the central area, with ornate, curved corner pieces at each of the four corners. The word "TOPOLOGY" is centered in the middle of the page in a white, serif, all-caps font.

# TOPOLOGY

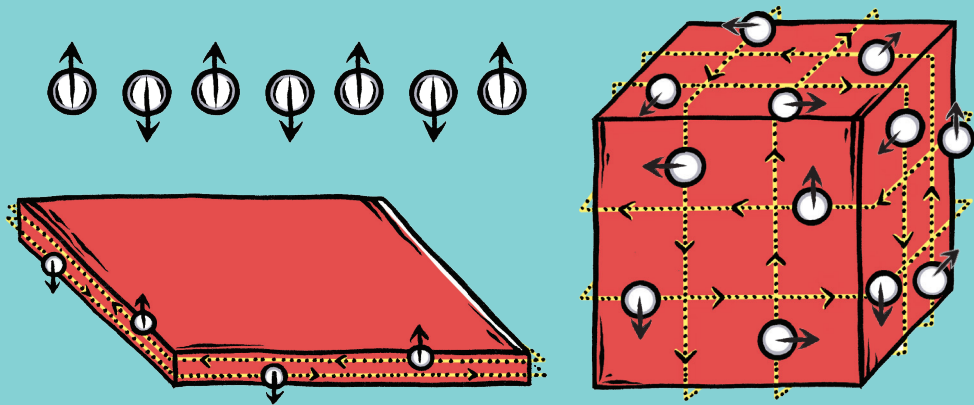


## NOBEL PRIZE, 2016

For theoretical discoveries of topological phase transitions and topological phases of matter.

The image features a solid teal background. A white decorative border frames the central area, with ornate, curved corner pieces at each of the four corners. The word "TOPOLOGY" is centered in the middle of the page in a white, serif, all-caps font.

# TOPOLOGY



## NOWADAYS

This work opened the route to the discovery of many new topological states in matter at one, two or three dimensions in magnets, metals or insulators.

The image features a solid teal background. A white decorative border frames the central area, with ornate, curved corner pieces at each of the four corners. The word "TOPOLOGY" is centered in the middle of the page in a white, serif, all-caps font.

# TOPOLOGY